Acta Crystallographica Section F
Structural Biology and Crystallization Communications
ISSN 1744-3091

Structure of the GDP-bound G domain of the RGK protein Rem2

Philippe Reymond,[a,b] Aline Coquard,[a] Mélanie Chenon,[a] Mahel Zeghouf,[a] Ahmed El Marjou,[c,d] Andrew Thompson[e] and Julie Ménétrey[a]*

[a]Laboratoire d'Enzymologie et Biochimie Structurales, Centre de Recherche de Gif, CNRS, 91198 Gif-sur-Yvette, France, [b]ED 387 iViv, Université Pierre et Marie Curie, 75005 Paris, France, [c]Institut Curie, Centre de Recherche, 75248 Paris, France, [d]CNRS UMR144, 26 Rue d'Ulm, 75248 Paris, France, and [e]Synchrotron SOLEIL, L'Orme des Merisiers, BP 48 St Aubin, 91192 Gif-sur-Yvette, France

Correspondence e-mail: julie.menetrey@lebs.cnrs-gif.fr

Received 22 February 2012
Accepted 28 March 2012

PDB Reference: Rem2 G domain bound to GDP, 4aii.

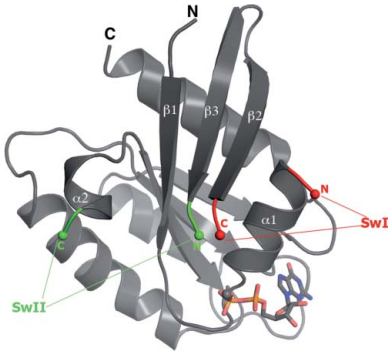

RGK proteins are atypical small GTP-binding proteins that are involved in the regulation of voltage-dependent calcium channels and actin cytoskeleton remodelling. The structure of the Rem2 G domain bound to GDP is reported here in a monoclinic crystal form at 2.66 Å resolution. It is very similar to the structure determined previously from an orthorhombic crystal form. However, differences in the crystal-packing environment revealed that the switch I and switch II regions are flexible and not ordered as previously reported. Comparison of the available RGK protein structures along with those of other small GTP-binding proteins highlights two structural features characteristic of this atypical family and suggests that the conserved tryptophan residue in the D*X*WE*X* motif may be a structural determinant of the nucleotide-binding affinity.

1. Introduction

The RGK (**R**ad, **G**em/**K**ir) family consists of four related proteins within the small GTP-binding protein superfamily: Rad, Gem, Rem1 and Rem2. RGK proteins have been shown to control the activity of voltage-dependent Ca^{2+} channels by interacting with their accessory β-subunits (Béguin *et al.*, 2001; Finlin *et al.*, 2003, 2005, 2006), in addition to regulating Rho signalling pathways to modulate actin cytoskeleton remodelling (Ward *et al.*, 2002; Aresta *et al.*, 2002; Hatzoglou *et al.*, 2007; for reviews, see Correll *et al.*, 2008; Flynn & Zamponi, 2010).

RGK proteins are comprised of a central G domain flanked by unique N-terminal and C-terminal extensions. The N-terminal extension varies from 44 to 88 residues and shares 7% sequence similarity, while the C-terminal extension is shorter at 29–37 residues and shares 40% sequence similarity. While the N-terminal extension has no identified sequence motif, the C-terminal extension binds calmodulin in a calcium-dependent manner (Fischer *et al.*, 1996; Moyers *et al.*, 1997; Béguin *et al.*, 2005; Correll *et al.*, 2007). The G domain of RGK proteins is more conserved and shares 52% sequence similarity. Typical small GTP-binding G domains contain five conserved motifs (G1–G5) that are essential for nucleotide binding and GTP hydrolysis. Critical substitutions have been identified in these motifs among RGK proteins, and two of these are critical to promote conformational changes of the switch regions during the GDP/GTP cycle. Firstly, RGK proteins lack the highly conserved threonine residue within switch I (G1 motif; Thr35 in H-Ras) that binds to the GTP γ-phosphate and magnesium ions; these interactions trigger switch I rearrangement. It should be noted that the switch I sequence is not conserved among RGK proteins. Secondly, RGK proteins exhibit a conserved D*X*WE*X* motif (G3 motif) at the beginning of switch II that diverges significantly from the DTAGQ motif found in other small GTP-binding proteins. The glycine residue in the DTAGQ motif is responsible for the switch II rearrangement on GTP binding by sensing the GTP γ-phosphate. Biochemical studies have revealed that all RGK proteins bind both GDP and GTP with micromolar affinity (Reynet & Kahn, 1993; Maguire *et al.*, 1994;

Table 1
Data-collection and refinement statistics.

Values in parentheses are for the highest resolution shell.

Crystal system	
Space group	$P2_1$
Unit-cell parameters (Å, °)	a = 50.92, b = 59.37, c = 57.30, β = 101.51
Diffraction data	
Resolution range (Å)	41.65–2.66 (2.80–2.66)
Reflections recorded	36695
Unique reflections	9624
R_{meas} (%)	11.3 (40.9)
$\langle I/\sigma(I)\rangle$	5.7 (2.0)
Completeness (%)	98.8 (98.8)
Final model	
R_{cryst} (%)	24.7
R_{free}† (%)	32.4
R.m.s. deviation from ideality	
Bond lengths (Å)	0.214
Bond angles (°)	1.867
Contents of asymmetric unit	
Protein molecules	2
Protein atoms	2295
Water atoms	12
Ligand atoms	58
Mean B factor by atom type (Å^2)	
Protein	35.67
Water	30.26
Ligands	32.94
Ramachandran plot, residues in (%)	
Favoured region	91.2
Allowed region	8.8
Outlier region	0.0
PDB code	4aii

† R_{free} was calculated using 5% of data excluded from refinement.

Finlin & Andres, 1997; Opatowsky *et al.*, 2006; Yanuar *et al.*, 2006; Splingard *et al.*, 2007; Sasson *et al.*, 2011). Together, these primary-sequence substitutions suggest that although they bind guanine nucleotides, RGK proteins may not behave as canonical small GTP-binding proteins, raising questions about their ability to adopt different conformations during the GDP/GTP cycle.

Here, we report the structure of the GDP-bound G domain of Rem2 in a monoclinic crystal form that sheds new light on the flexibility of the switch I and II regions. An overall structural analysis of RGK proteins unveils characteristic features of these atypical small GTP-binding proteins and suggests that the conserved tryptophan residue in the D*X*WE*X* motif may be a structural determinant for the nucleotide-binding affinity.

2. Materials and methods

2.1. Protein expression and purification

The rat Rem2 gene was kindly supplied by Dr Jean De Gunzburg (Institut Curie, France). The G domain corresponding to residues Asp113–Gly283, hereafter called Rem2_Gdomain, was amplified by PCR. The PCR product was digested with *Nde*I and *Xho*I, subcloned into pET-21a(+) (Novagen) and expressed in *Escherichia coli* BL21-Gold(DE3) cells. Rem2_Gdomain was produced as an uncleavable six-His-tag fusion protein encompassing the sequence MHHH-HHHGG before residue Asp113 of Rem2. The soluble lysate was loaded onto an Ni^{2+}–NTA (Amersham Biosciences) column equilibrated with 50 m*M* Tris–HCl pH 8, 300 m*M* NaCl, 20 m*M* imidazole, 2 m*M* $MgCl_2$, 2 m*M* β-mercaptoethanol. After washing, the protein was eluted with a gradient of increasing imidazole concentration (to 250 m*M*). The protein solution was dialyzed against buffer *A* (50 m*M* Tris–HCl pH 8, 50 m*M* NaCl, 5 m*M* $MgCl_2$, 2 m*M* β-mercaptoethanol) and loaded onto a Q-Sepharose (Amersham Biosciences) column equilibrated with the same buffer. The protein was then eluted with a linearly increasing NaCl concentration gradient. The fractions containing the protein were collected and concentrated to ~20 mg ml^{-1}. The final preparation was stored at 193 K in 50 m*M* Tris–HCl pH 8, 150 m*M* NaCl, 5 m*M* $MgCl_2$, 2 m*M* β-mercaptoethanol with the addition of 2 m*M* GDP and was >95% pure as assessed by SDS–PAGE.

2.2. Crystallization, data collection and structure determination

Crystals of Rem2_Gdomain bound to GDP were grown in sitting drops consisting of equal volumes of protein solution (20 mg ml^{-1}) and reservoir solution (13.5% PEG 4000, 10% 2-propanol, 100 m*M* HEPES sodium salt pH 7.4) by the vapour-diffusion method at 290 K. Seeding techniques were applied to obtain single crystals. Crystals were briefly transferred into a cryoprotectant composed of reservoir solution supplemented with 20% ethylene glycol and cooled in liquid nitrogen. Diffraction data were collected at 100 K on beamline PROXIMA1 at the SOLEIL synchrotron. The crystals diffracted to 2.66 Å resolution and belonged to the primitive monoclinic space group $P2_1$, with two molecules (*A* and *B*) per asymmetric unit. X-ray data were integrated and scaled with *XDS* (Kabsch, 2010). The structure was determined by molecular replacement with *Phaser* (McCoy *et al.*, 2007) using the structure of human Rem2_Gdomain–GDP (PDB entry 3cbq; Structural Genomics Consortium, unpublished work) as a search model. The switch regions (140–150 and 174–189 in the rat sequence) were omitted from the model for molecular replacement. Refinement was then carried out with *REFMAC*5 (Murshudov *et al.*, 2011) from *CCP*4 (Winn *et al.*, 2011) using NCS restraints between molecules *A* and *B*, with the exception of their switch regions (137–149 and 173–189). The final model included residues 113–136, 151–170 and 183–282 in molecule *A*, and residues 113–137, 150–170 and 183–282 in molecule *B*. Graphical model building was performed with *Coot* (Emsley & Cowtan, 2004). Crystallographic statistics are presented in Table 1. Figures were produced using *PyMOL* (DeLano, 2002).

2.3. Size-exclusion chromatography coupled with multi-angle laser light scattering

Rem2_Gdomain–GDP was analysed by size-exclusion chromatography (SEC) on a Shodex Protein KW-803 column (Phenomenex) at 279 K in buffer consisting of 50 m*M* Tris pH 7.5, 150 m*M* NaCl, 2 m*M* $MgCl_2$ using a Shimadzu Prominence HPLC. Multi-angle laser light scattering (MALLS) was measured with a MiniDAWN TREOS (Wyatt Technology). Refractometry was monitored using an Optilab T-rEX (Wyatt Technology) and dynamic light scattering with a WyattQELS (Wyatt Technology). The data were analysed using *ASTRA* 6 software (Wyatt Technology). A 0.183 ml g^{-1} refractive-index increment, d*n*/d*C*, was used to calculate the protein concentration from the refractive-index measurements.

3. Results and discussion

3.1. Overall structure and oligomeric state determination

The structure of the G domain of rat Rem2 (Rem2_Gdomain; residues 113–283) bound to GDP was determined at 2.66 Å resolution (PDB entry 4aii; statistics are given in Table 1) with two molecules (*A* and *B*) in the asymmetric unit. No defined electron density was observed in the switch I and II regions, *i.e.* residues 137–150 and 171–182 of molecule *A*, and residues 138–149 and 171–182 of molecule *B*. In particular, the D*X*WE*X* motif (residues 170–174) had

no density after the conserved aspartate residue. There are no significant differences between molecules *A* and *B*, and their entire C^{α} traces show an r.m.s. deviation of just 0.043 Å (calculated on 130 residues excluding the switch regions). In the Rem2_Gdomain–GDP structure Rem2 possesses the G-domain fold typical of the Ras superfamily, with a central six-stranded β-sheet (strands $\beta1$–$\beta6$) flanked by five α-helices ($\alpha1$–$\alpha5$) (Fig. 1*a*). The nucleotide-binding site reveals the classical fold, with the magnesium ion possessing an octahedral coordination shell that includes four water molecules, one β-phosphate O atom and the side chain of Ser129 (Ser17 of H-Ras) from the G1 motif.

In the crystal, molecules *A* and *B* interact through their respective $\alpha3$–$\beta4$ loops, making two main chain–main chain hydrogen bonds between residues His220 and Asp222. In addition, a patch of four histidines is formed at the interface by His220 and His221 from each molecule. Because of these interactions, we postulated that Rem2_Gdomain could be a dimer. In order to evaluate the oligomeric state of Rem2_G domain–GDP in solution, we performed SEC-MALLS experiments. Rem2_Gdomain–GDP was analyzed at four different concentrations from 4.6 to 29 mg ml^{-1}. At all of the concentration tested, a single peak was observed with a weight-averaged mass of about 20.0–21.0 kDa (±0.6%; Fig. 1*b*). The theoretical mass of Rem2_Gdomain is 20.1 kDa; thus, the SEC-MALLS experiments revealed that Rem2_G domain–GDP is a monomer in solution.

3.2. The switch conformations

The G domains of Rem2 from rat and human bound to GDP have been crystallized in a primitive monoclinic ($P2_1$) form with two molecules in the asymmetric unit (this study) and a centred orthorhombic ($C222_1$) form with one molecule in the asymmetric unit (PDB entry 3cbq; Structural Genomics Consortium, unpublished work), respectively. Structural comparison of these two crystal forms revealed that the overall folds and the MgGDP-binding sites of Rem2 are virtually identical to each other (r.m.s.d. of 0.51 Å on 130 C^{α} atoms, excluding switch regions; Fig. 1*c*). However, differences are observed in the switch regions, which have well defined

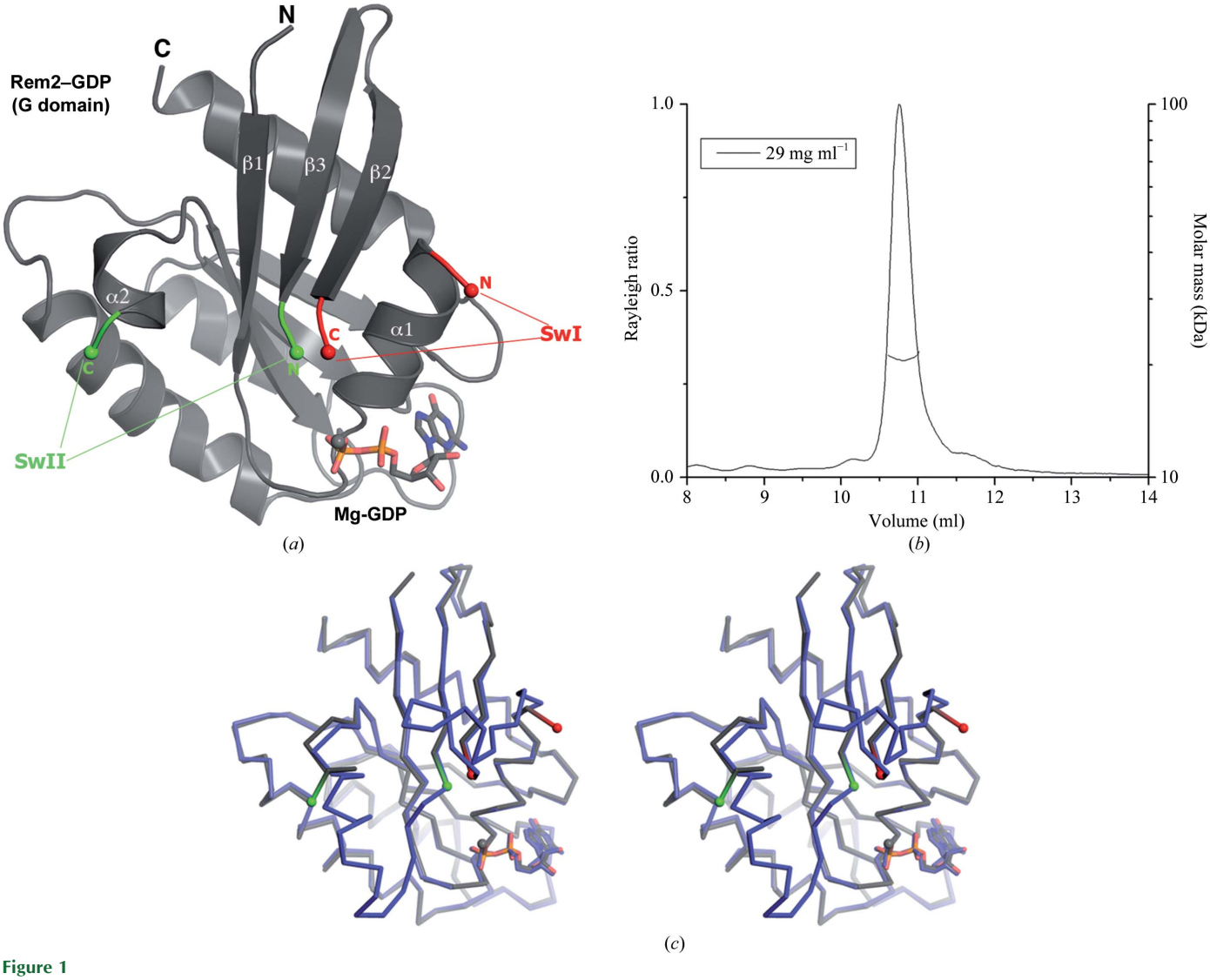

Figure 1
Structural characterization of the G domain of Rem2 bound to GDP. (*a*) Structure of the monoclinic crystal form. The N- and C-termini of switches I and II are shown in red and green, respectively. (*b*) SEC-MALLS analysis of Rem2_Gdomain–GDP at 29 mg ml^{-1}. The size-exclusion profiles of the protein (monitored by refractometry) and the molecular masses (calculated from light-scattering and refractometry data) are plotted. (*c*) A cross-eye stereoview of the superposition of Rem2–GDP in the monoclinic (black, this study) and orthorhombic (blue, PDB entry 3cbq) crystal forms. Note the well defined conformation of switches I and II in the orthorhombic form.

Table 2
Crystallographic information from crystal structures of the G domains of RGK proteins bound to GDP.

	PDB code	Resolution (Å)	Space group	Unit-cell parameters				Molecules in asymmetric unit	Reference
				a (Å)	*b* (Å)	*c* (Å)	*β* (°)		
Rad	2dpx	1.80	$P2_1$	52.16	58.61	53.44	97.98	2	Yanuar *et al.* (2006)
	2gjs	1.90	$P2_1$	51.43	58.56	53.60	97.18	2	Structural Genomics Consortium (unpublished work)
Gem	2cjw	2.10	$P6_1$	116.68	116.62	81.41	90.00	2	Splingard *et al.* (2007)
	2g3y	2.40	$P4_32_12$	51.24	51.24	173.87	90.00	1	Structural Genomics Consortium (unpublished work)
	2ht6	2.40	$P2_12_12_1$	39.84	81.43	124.10	90.00	2	Opatowsky *et al.* (2006)
Rem1	2nzj	2.50	$P2_12_12_1$	43.64	102.28	165.57	90.00	4	Structural Genomics Consortium (unpublished work)
Rem2	3cbq	1.82	$C222_1$	64.14	64.33	73.20	90.00	1	Structural Genomics Consortium (unpublished work)
	4aii	2.66	$P2_1$	50.92	59.37	57.30	101.51	2	This study

conformations in the Rem2–GDP molecule in the orthorhombic form, while our monoclinic form shows no electron density for these regions in both molecules (Fig. 1*c*). The absence of electron density suggests that switches I and II are disordered. Crystal-packing environment analysis of the orthorhombic form revealed that both switch I and switch II are stabilized by two symmetry molecules through hydrogen bonds and either hydrophobic or van der Waals interactions. In the case of the monoclinic form no symmetry molecules are found in the close vicinity of the switch regions. Overall, our structure reveals that switch I and switch II of Rem2 are flexible regions in the GDP-bound form and in the absence of the N- and C-terminal extensions.

To date, seven structures of the G domains from the four RGK proteins are available in the Protein Data Bank (PDB), providing 12 refined molecules for structural comparison (Yanuar *et al.*, 2006; Opatowsky *et al.*, 2006; Splingard *et al.*, 2007; Table 2 and Fig. 2). Note that two structures of the Rad G domain (PDB entries 2dpx and 2cjw) were determined in the same crystal form, but only the 2dpx structure, which has the better resolution, was used in structural comparison (Table 2). The overall fold of Rem2 is very similar to those of other RGK proteins bound to GDP, with an average r.m.s. deviation ranging from 0.63 and 0.65 Å for Rad and Gem to 0.69 Å for Rem1 (calculated on 109 C^{α} atoms, excluding the switch regions, the α3 helix and the α3–β5 loop). Small structural variations are observed for the α3 helix and α3–β5 loop among RGK proteins (in the Gem 2g3y and Rem1 2nzj molecules *C* and *D* compared with the other RGK molecules) mainly owing to crystal-packing contacts. However, the switch I and II regions exhibit differences among the RGK G-domain structures. Both switch I and switch II are either completely modelled, partially modelled or not modelled at all. A careful analysis of the crystal-packing environment in all of these structures revealed that switch I and II regions that are completely or partially modelled make contacts with symmetry molecules. In addition, RGK protein structures for which two or more crystal forms are available, as for Rem2 or Gem (see Table 2), revealed that the switch regions exhibit different conformations for the same protein. Overall, our analysis supports the idea that the crystal-packing environment stabilizes or imposes a conformation on the switch regions and that the switch regions are disordered in the absence of contact. Together, these observations suggest that in the absence of their N- and C-terminal extensions the switch I and switch II regions of the GDP-bound forms of RGK proteins are flexible.

3.3. Structural features of the RGK protein G domain

Structural comparison of the RGK proteins along with other small GTP-binding proteins emphasizes two structural features of the GDP-bound form that we have previously reported for Gem (Splingard *et al.*, 2007). Firstly, the beginning of switch II encompassing the D*X*WE*X* motif (G3 motif) is arranged differently from that in H-Ras (Fig. 3). Indeed, owing to a drastic rotation of the backbone dihedral ψ angle ($\Delta\psi \simeq 150^{\circ}$) at position 2 of the D*X*WE*X* motif, the residue side chains at position 2 (methionine, isoleucine or threonine) and position 3 (tryptophan) are flipped compared with the equivalent threonine and alanine residues in H-Ras (Figs. 3*a* and 3*b*). In this conformation, the tryptophan residue lies in a pocket composed of hydrophobic residues from the β1 strand and the α2 and α3 helices (Fig. 3*c*). Since this structural feature is observed in the four RGK proteins, we suspect that it probably results from the presence of the tryptophan residue at position 3, which is strictly

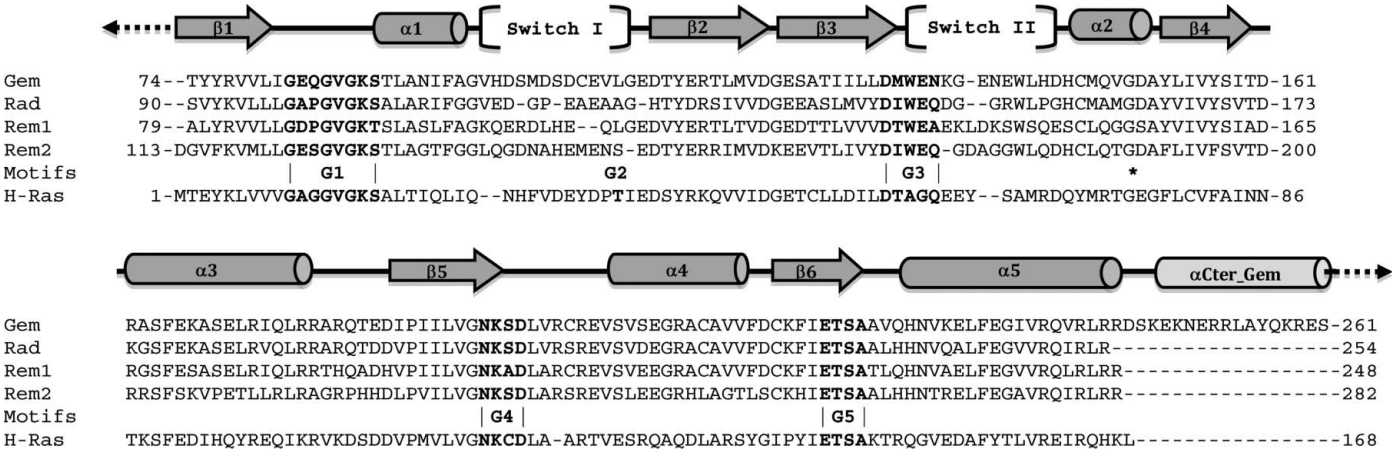

Figure 2
Sequence alignment based on crystal structures of the G domains of RGK proteins. Human Gem, Rad and Rem1 and rat Rem2 sequences were used.

conserved. In several RGK structures the tryptophan residue has no defined electron density, suggesting that it is flexible; it thus can occupy the classical position observed for the equivalent alanine side chain in H-Ras. Modelling the tryptophan in this classical conformation revealed that its bulky side chain should disturb the water-coordination shell of the magnesium ion and thus the magnesium ion and the nucleotide (Fig. 3*d*). This assumption could explain the low affinity of RGK proteins for nucleotides (Reynet & Kahn, 1993; Maguire *et al.*, 1994; Finlin & Andres, 1997; Opatowsky *et al.*, 2006; Yanuar *et al.*, 2006; Splingard *et al.*, 2007; Sasson *et al.*, 2011).

The second structural feature is the rearrangement of the β2 strand at the end of switch I compared with H-Ras (Fig. 3*a*). Drastic rotations in the φ–ψ dihedral angles are observed at residue Asp151 in the β2 strand in Rem2 (equivalent to Asp112, His125 and Asp115 in Gem, Rad and Rem1, respectively, and Asp38 in H-Ras) that shorten the strand at its N-terminus compared with H-Ras (Fig. 3*a*). This is probably a consequence of the atypical conformation of the D*X*WE*X* motif in switch II, since steric hindrance would occur between its backbone, especially that of the residue at position 2 and that of the classical β2 strand conformation observed in H-Ras (Fig. 3*a*). Together, these two conserved structural features in RGK proteins prevent switch I from folding back on the nucleotide as observed in H-Ras.

RGK proteins are small GTP-binding proteins with atypical primary-sequence and structural features. The structural data available for GDP-bound RGK proteins revealed that the switch regions are flexible in the absence of the N- and C-terminal extensions. The conserved tryptophan residue in the D*X*WE*X* motif of switch II is either stabilized in a hydrophobic pocket or is flexible. In the latter case, the tryptophan can come close to and disturb the water-

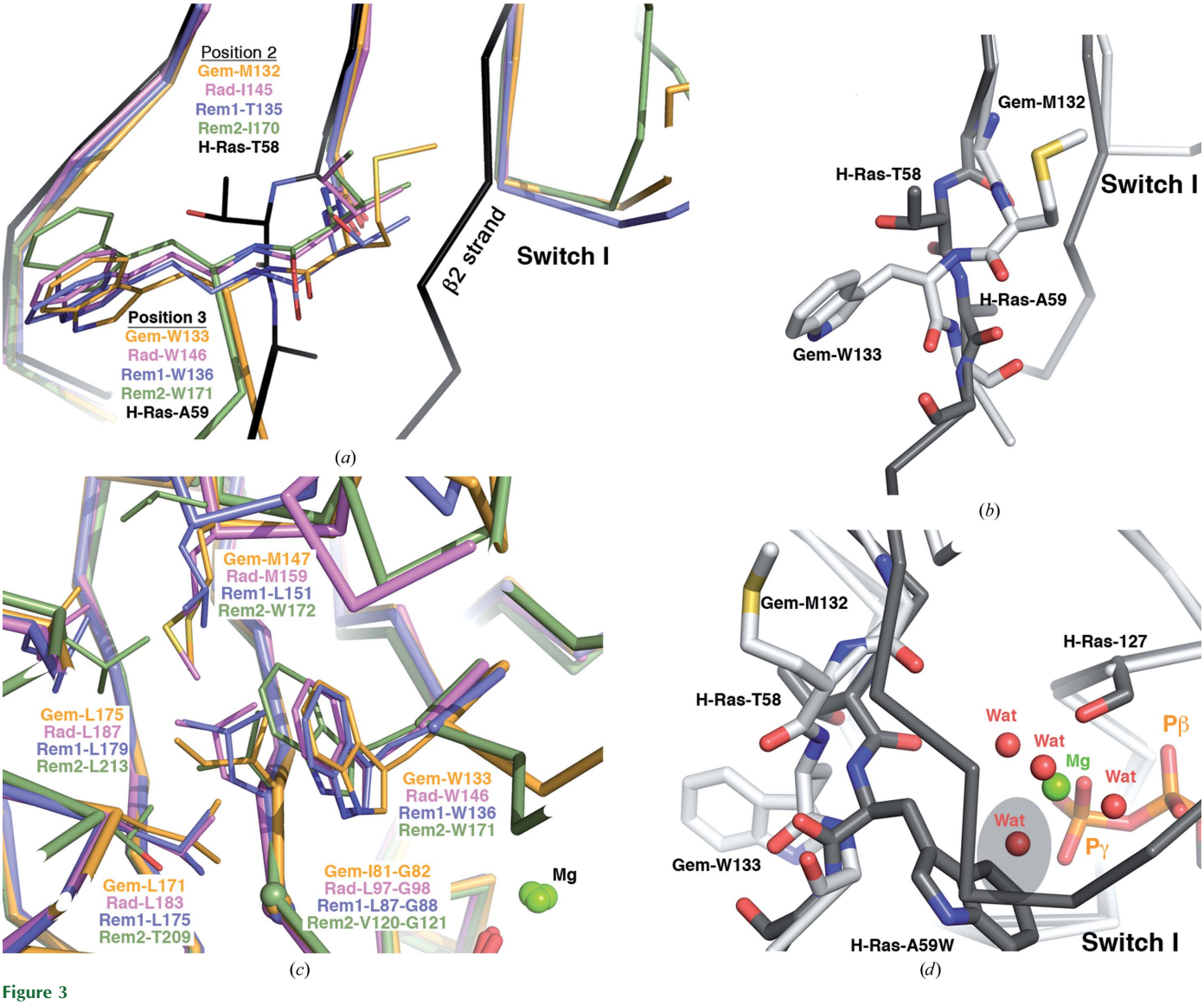

Figure 3
Structural features of the GDP-bound G domains of the RGK proteins. (*a*) Superposition between the H-Ras protein (PDB entry 4q21; Milburn *et al.*, 1990; shown in black) and the four RGK proteins (shown in colours). Gem (PDB entry 2cjw), Rad (PDB entry 2dpx), Rem1 (2nzj) and Rem2 (PDB entry 3cbq) are shown in orange, violet, blue and green, respectively. The residues at positions 2 and 3 of the G3 motif (DTAGQ in H-Ras and D*X*WE*X* in RGK) are indicated in stick representation. Note that human sequence numbering is used for Rem2. (*b*) A close-up view of the G3 motif of Gem (PDB entry 2cjw; only one RGK protein is indicated for clarity) compared with H-Ras (PDB entry 4q21) is shown with residues at positions 2 and 3 indicated in stick representation. (*c*) The hydrophobic pocket surrounding the conserved G3 motif tryptophan. A superposition of the four RGK proteins is shown as defined in (*a*). (*d*) A close-up view of the nucleotide pocket of H-Ras (PDB entry 4q21) is shown with Ala59 from the G3 motif modelled as a tryptophan. For comparison, Gem (PDB entry 2cjw; only one RGK protein is indicated for clarity) is shown superposed with H-Ras. The grey area indicates the steric hindrance between the modelled tryptophan of H-Ras and the water-coordination shell of the magnesium ion

coordination shell of the magnesium ion. Further investigation is required in order to elucidate the role of this conserved tryptophan as a structural determinant for the nucleotide-binding affinity.

We thank Valérie Campanacci, Christophe Velours and Davy Martin for help with the SEC-MALLS experiments. This work benefited from the facilities of the IMAGIF platform (http://www.imagif.cnrs-gif.fr), providing access to the TECAN crystallization robot. X-ray data collection was performed with the help of the staff of the PROXIMA1 beamline at the SOLEIL synchrotron (Saint-Aubin, France). This work was supported by a grant from ANR (ANR-08-JCJC-0110-01) to JM.

References

Aresta, S., de Tand-Heim, M.-F., Béranger, F. & de Gunzburg, J. (2002). *Biochem. J.* **367**, 57–65.
Béguin, P., Mahalakshmi, R. N., Nagashima, K., Cher, D. H., Kuwamura, N., Yamada, Y., Seino, Y. & Hunziker, W. (2005). *Biochem. J.* **390**, 67–75.
Béguin, P., Nagashima, K., Gonoi, T., Shibasaki, T., Takahashi, K., Kashima, Y., Ozaki, N., Geering, K., Iwanaga, T. & Seino, S. (2001). *Nature (London)*, **411**, 701–706.
Correll, R. N., Pang, C., Finlin, B. S., Dailey, A. M., Satin, J. & Andres, D. A. (2007). *J. Biol. Chem.* **282**, 28431–28440.
Correll, R. N., Pang, C., Niedowicz, D. M., Finlin, B. S. & Andres, D. A. (2008). *Cell. Signal.* **20**, 292–300.
DeLano, W. L. (2002). *PyMOL*. http://www.pymol.org.
Emsley, P. & Cowtan, K. (2004). *Acta Cryst.* D**60**, 2126–2132.
Finlin, B. S. & Andres, D. A. (1997). *J. Biol. Chem.* **272**, 21982–21988.
Finlin, B. S., Correll, R. N., Pang, C., Crump, S. M., Satin, J. & Andres, D. A. (2006). *J. Biol. Chem.* **281**, 23557–23566.
Finlin, B. S., Crump, S. M., Satin, J. & Andres, D. A. (2003). *Proc. Natl Acad. Sci. USA*, **100**, 14469–14474.
Finlin, B. S., Mosley, A. L., Crump, S. M., Correll, R. N., Ozcan, S., Satin, J. & Andres, D. A. (2005). *J. Biol. Chem.* **280**, 41864–41871.
Fischer, R., Wei, Y., Anagli, J. & Berchtold, M. W. (1996). *J. Biol. Chem.* **271**, 25067–25070.
Flynn, R. & Zamponi, G. W. (2010). *Channels*, **4**, 3–8.
Hatzoglou, A., Ader, I., Splingard, A., Flanders, J., Saade, E., Leroy, I., Traver, S., Aresta, S. & de Gunzburg, J. (2007). *Mol. Biol. Cell*, **18**, 1242–1252.
Kabsch, W. (2010). *Acta Cryst.* D**66**, 125–132.
Maguire, J., Santoro, T., Jensen, P., Siebenlist, U., Yewdell, J. & Kelly, K. (1994). *Science*, **265**, 241–244.
McCoy, A. J., Grosse-Kunstleve, R. W., Adams, P. D., Winn, M. D., Storoni, L. C. & Read, R. J. (2007). *J. Appl. Cryst.* **40**, 658–674.
Milburn, M. V., Tong, L., deVos, A. M., Brünger, A., Yamaizumi, Z., Nishimura, S. & Kim, S.-H. (1990). *Science*, **247**, 939–945.
Moyers, J. S., Bilan, P. J., Zhu, J. & Kahn, C. R. (1997). *J. Biol. Chem.* **272**, 11832–11839.
Murshudov, G. N., Skubák, P., Lebedev, A. A., Pannu, N. S., Steiner, R. A., Nicholls, R. A., Winn, M. D., Long, F. & Vagin, A. A. (2011). *Acta Cryst.* D**67**, 355–367.
Opatowsky, Y., Sasson, Y., Shaked, I., Ward, Y., Chomsky-Hecht, O., Litvak, Y., Selinger, Z., Kelly, K. & Hirsch, J. A. (2006). *FEBS Lett.* **580**, 5959–5964.
Reynet, C. & Kahn, C. R. (1993). *Science*, **262**, 1441–1444.
Sasson, Y., Navon-Perry, L., Huppert, D. & Hirsch, J. A. (2011). *J. Mol. Biol.* **413**, 372–378.
Splingard, A., Ménétrey, J., Perderiset, M., Cicolari, J., Regazzoni, K., Hamoudi, F., Cabanié, L., El Marjou, A., Wells, A., Houdusse, A. & de Gunzburg, J. (2007). *J. Biol. Chem.* **282**, 1905–1915.
Ward, Y., Yap, S.-F., Ravichandran, V., Matsumura, F., Ito, M., Spinelli, B. & Kelly, K. (2002). *J. Cell Biol.* **157**, 291–302.
Winn, M. D. *et al.* (2011). *Acta Cryst.* D**67**, 235–242.
Yanuar, A., Sakurai, S., Kitano, K. & Hakoshima, T. (2006). *Genes Cells*, **11**, 961–968.